Influence of local carrying capacity restrictions on stochastic predator–prey models

2007 J. Phys.: Condens. Matter 19 065139

(http://iopscience.iop.org/0953-8984/19/6/065139)

INSTITUTE OF PHYSICS PUBLISHING JOURNAL OF PHYSICS: CONDENSED MATTER

J. Phys.: Condens. Matter **19** (2007) 065139 (14pp) doi:10.1088/0953-8984/19/6/065139

Influence of local carrying capacity restrictions on stochastic predator–prey models

Mark J Washenberger[1], Mauro Mobilia[2] and Uwe C Täuber[1]

[1] Department of Physics and Center for Stochastic Processes in Science and Engineering, Virginia Polytechnic Institute and State University, Blacksburg, VA 24061-0435, USA
[2] Arnold Sommerfeld Center for Theoretical Physics and Center for NanoScience, Department of Physics, Ludwig-Maximilians-Universität München, D-80333 Munich, Germany

E-mail: mwashenb@vt.edu, mauro.mobilia@physik.lmu.de and tauber@vt.edu

Received 30 June 2006, in final form 6 September 2006
Published 22 January 2007
Online at stacks.iop.org/JPhysCM/19/065139

Abstract

We study a stochastic lattice predator–prey system by means of Monte Carlo simulations that do not impose any restrictions on the number of particles per site, and discuss the similarities and differences of our results with those obtained for site-restricted model variants. In accord with the classic Lotka–Volterra mean-field description, both species always coexist in two dimensions. Yet competing activity fronts generate complex, correlated spatio-temporal structures. As a consequence, finite systems display transient erratic population oscillations with characteristic frequencies that are renormalized by fluctuations. For large reaction rates, when the processes are rendered more local, these oscillations are suppressed. In contrast with the site-restricted predator–prey model, we also observe species coexistence in one dimension. In addition, we report results on the steady-state prey age distribution.

(Some figures in this article are in colour only in the electronic version)

1. Introduction

Originally devised to describe autocatalytic chemical reactions [1] and fish harvests in the Adriatic [2], the classic Lotka–Volterra coupled set of ordinary differential equations represents a central paradigm for the emergence of species coexistence and periodic oscillations in nonlinear systems with competing constituents. It thus features prominently in textbooks on nonlinear dynamics [3], ecology [4, 5], population dynamics [6, 7], and mathematical biology [8], although this *deterministic* rate equation system is known to be mathematically unstable against modifications, spatial variations, and stochasticity, and therefore also unlikely to be biologically relevant [7, 8].

Neither criticism however pertains to *stochastic* spatial predator–prey models [9–24], for which the mean-field approximation recovers the original Lotka–Volterra differential equations.

In stark contrast with the deterministic Lotka–Volterra rate equations, such stochastic lattice predator–prey models in fact display remarkably robust features (for a recent overview, see [24]): sufficiently deep in the species coexistence phase, the population densities oscillate in an irregular manner, however with characteristic periods and amplitudes that vanish in the thermodynamic limit [13, 15–17, 20, 21, 23, 24]; these erratic oscillations are induced by recurrent activity waves that initially form concentric rings, and upon merging produce complex spatiotemporal structures [11, 19, 23, 24].

These quite generic characteristics are found in computer simulations of several distinct model variants, differing in the precise microscopic algorithmic set-ups such as the number of possible states per lattice site and detailed implementations of the reaction scheme, e.g., parallel versus sequential updates, etc. Perhaps surprisingly this includes even long-range processes [16, 17], generalizations to 'smart' predators and prey who respectively follow/evade the other species [11, 14], and a variation where the predation reaction is split up into two separate and independent processes [23]. Indeed, already a zero-dimensional stochastic predator–prey model exhibits prominent population oscillations driven by the inevitable internal reaction noise [22]; such finite-size fluctuations also drastically affect the properties of, e.g., the three-species cyclic Lotka–Volterra model [25].

Largely for computational simplicity, such lattice models for reacting particle systems typically operate with constraints on the possible site occupation numbers, usually allowing only at most one particle per site; but four-state predator–prey systems which permit both a single predator and prey per site have been studied too [15, 16, 20]. Biologically and ecologically, such site occupation number restrictions may be interpreted as originating in *local* limitations on resources for either species. On the mean-field description level, they are represented by finite carrying capacities in the rate equations that prevent unbounded (Malthusian) species growth (see, e.g., [7, 8]). Already on this rate equation level, such constraints have a dramatic effect: they lead to the emergence of an extinction threshold for the predator population. In the stochastic spatial system (and in the thermodynamic limit), predator extinction is governed by a continuous active-to-absorbing phase transition. As one would expect [26–29], the associated critical exponents are those of directed percolation [10, 11, 14–17, 20, 21]; an analytic argument that demonstrates this assertion, based on a field theory representation of the underlying stochastic processes (see, e.g., [29]), is presented in [24].

Presumably already a lattice representation should be viewed as a mesoscopic representation of the chemical or biological system under consideration; naturally, therefore, the question arises of what influence the implicit coarse-graining scale might have on the system's properties. Also, it is of interest to study a stochastic spatial system most closely related to the original Lotka–Volterra model, i.e. without any limits on the carrying capacities (specifically for the prey). In this work, we investigate such an unconstrained lattice predator–prey model. As suggested by the corresponding mean-field theory, we do not encounter predator extinction, but both species always coexist (within the typical timescales of our simulation runs). This appears to be true even in one dimension. The strictly periodic population oscillations, which are moreover determined by the initial configuration, of the deterministic rate equations are replaced with erratic, transient oscillations largely determined by the intrinsic rates, and with frequencies renormalized by the fluctuations. If the reaction rates are high, and the processes effectively rendered more local, we find the oscillatory behaviour to cease. As in the lattice models with site occupation number restrictions, persistent complex spatio-temporal structures form, but the activity fronts are generally more diffuse.

In the following section, we briefly review the results of the mean-field rate equation approximation for Lotka–Volterra type predator–prey models with and without limiting

carrying capacities. Next we describe the alterations in the Monte Carlo algorithm and data structure that are required if we wish to allow arbitrarily many occupants per lattice site, before we present our simulation results. Finally, we summarize and discuss our findings in the concluding section.

2. Model and mean-field rate equations

2.1. Unconstrained Lotka–Volterra rate equations

We wish to consider a two-species system of diffusing particles or population members subject to the following reactions:

$$\begin{aligned} &A \to \emptyset, && \text{rate } \mu, \\ &A + B \to A + A, && \text{rate } \lambda, \\ &B \to B + B, && \text{rate } \sigma. \end{aligned} \tag{1}$$

The 'predators' A die spontaneously at rate $\mu > 0$, whereas the 'prey' B proliferate with rate $\sigma > 0$. In the absence of the binary 'predation' interaction with rate λ, the uncoupled first-order processes would naturally lead to predator extinction $a(t) = a(0)\mathrm{e}^{-\mu t}$, and Malthusian prey population explosion $b(t) = b(0)\mathrm{e}^{\sigma t}$. Here, $a(t)$ and $b(t)$ respectively denote the A/B concentrations or predator/prey population densities. The second reaction in the above scheme (1) induces species coexistence [1, 2].

All three reactions (1) as well as nearest–neighbour hopping are to be interpreted as *stochastic* processes, and the spatial distribution of reactants as well as reaction-induced correlations turn out to be relevant for a quantitative characterization of the kinetics of this system. Nevertheless, straightforward mean-field theory provides relevant insight into some basic properties of the system, and is reflected in the full stochastic simulation results to be discussed in section 4 below. Thus let us first ignore spatial variations, fluctuations and correlations, which leads to the corresponding *mean-field* rate equations for the average concentrations:

$$\dot{a}(t) = \lambda a(t)b(t) - \mu a(t), \qquad \dot{b}(t) = \sigma b(t) - \lambda a(t)b(t). \tag{2}$$

Setting the time derivatives to zero yields three stationary states $(a_\mathrm{s}, b_\mathrm{s})$:

(i) the absorbing state with total population extinction $(0, 0)$, which is obviously linearly unstable (if $\sigma > 0$);
(ii) predator extinction and prey explosion $(0, \infty)$, which for $\lambda > 0$ is also linearly unstable (and represents an absorbing state for the predators); and
(iii) species coexistence $(a_u = \sigma/\lambda, b_u = \mu/\lambda)$.

This fixed point is however only marginally stable, for the eigenvalues of the Jacobian stability matrix are purely imaginary, $\mathrm{i}\sqrt{\mu\sigma}$. Indeed, linearizing (2) near (a_u, b_u) results in the coupled differential equations $\delta\dot{a}(t) = \sigma\delta b(t)$, $\delta\dot{b}(t) = -\mu\delta a(t)$, which are readily solved by $\delta a(t) = \delta a(0)\cos(\sqrt{\mu\sigma}t) + \delta b(0)\sqrt{\sigma/\mu}\sin(\sqrt{\mu\sigma}t)$ and $\delta b(t) = -\delta a(0)\sqrt{\mu/\sigma}\sin(\sqrt{\mu\sigma}t) + \delta b(0)\cos(\sqrt{\mu\sigma}t)$.

This suggests periodic oscillations about the centre fixed point (a_u, b_u) with frequency $f = \sqrt{\mu\sigma}/2\pi$. Indeed, solving for the phase space trajectories yields $\mathrm{d}a/\mathrm{d}b = [a(\lambda b - \mu)]/[b(\sigma - \lambda a)]$, with a first integral (equal to the negative expression of the associated Lyapunov function for the rate equations with growth-limiting term, see below)

$$K(t) = \lambda[a(t) + b(t)] - \sigma \ln a(t) - \mu \ln b(t) \tag{3}$$

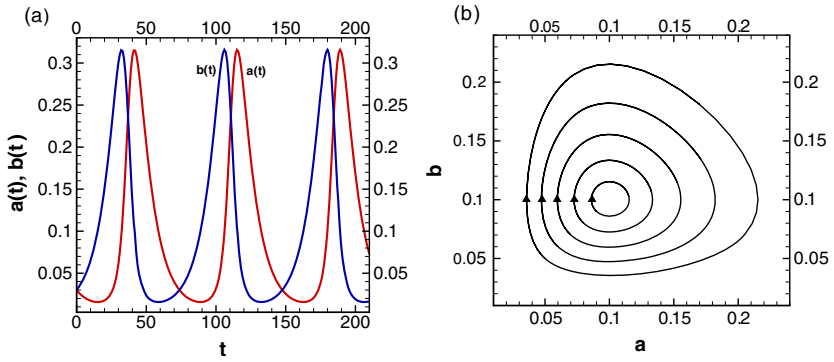

Figure 1. (a) Predator $a(t)$ (red) and prey $b(t)$ (blue) population oscillations resulting from the deterministic Lotka–Volterra equations (2), all computed with rates $\sigma = 0.1$, $\mu = 0.1$, and $\lambda = 1$. (b) Several periodic orbits in the a–b phase plane. The oscillatory kinetics is determined by the initial conditions.

that is conserved under the kinetics (2), $K(t) = K(0)$. The solutions of the *deterministic* mean-field Lotka–Volterra model are thus closed orbits in phase space, i.e. regular periodic nonlinear population oscillations whose amplitudes and frequencies depend crucially on the *initial* values $a(0)$ and $b(0)$, as depicted in figure 1. Notice however that there is no physical symmetry behind the conservation law (3); $K(t) = \text{const}$ is a mere mathematical property of the coupled mean-field rate equations, and will not hold for the underlying stochastic process.

2.2. Predator–prey rate equations with limited prey carrying capacity

These regular population oscillations fixed by the initial state are clearly not realistic in a biological setting. The Lotka–Volterra system is therefore often rendered 'more appropriate' through introducing a growth-limiting term for the prey [7, 8], whence the second differential equation in (2) is replaced with

$$\dot{b}(t) = \sigma b(t)\left[1 - \rho^{-1} b(t)\right] - \lambda a(t) b(t). \tag{4}$$

The new parameter $\rho > 0$ can be interpreted as the prey *carrying capacity* (maximum total population density). We remark in parentheses that the rate equations (2) and (4) may be derived in a systematic manner from the underlying stochastic master equation for the stochastic processes (1) with site occupation numbers restricted to 0 or 1 for either species [24].

The non-trivial stationary states in the ensuing restricted Lotka–Volterra model become modified to (ii) predator extinction and prey saturation $(0, \rho)$, linearly stable for $\lambda < \lambda_c = \mu/\rho$; and (iii) species coexistence (a_r, b_r) with $b_r = \mu/\lambda$ and $a_r = (\sigma/\lambda)(1 - \mu/\lambda\rho)$, which requires efficient predation, $\lambda > \lambda_c$. In this case the coexistence fixed point is always linearly stable, since the associated eigenvalues of the Jacobian, $\epsilon_\pm = -\sigma\mu(2\lambda\rho)^{-1}\left[1 \pm \sqrt{1 - 4\lambda\rho\sigma^{-1}\left(\lambda\rho\mu^{-1} - 1\right)}\right]$, have a negative real part indicating exponential approach to (a_r, b_r). For $\sigma > \sigma_s = 4\lambda\rho\,(\lambda\rho/\mu - 1) > 0$, or $\mu/\rho < \lambda < \lambda_s = \left(1 + \sqrt{1 + \sigma/\mu}\right)\mu/2\rho$, these eigenvalues are real, and the fixed point can be characterized as a stable node. On the other hand, if $\sigma < \sigma_s$ or $\lambda > \lambda_s$, i.e. deep in the coexistence phase, $\epsilon_\pm$ turn into a complex conjugate pair, and (a_r, b_r) becomes a stable spiral singularity, which is approached in a damped oscillatory manner. Actually, going beyond the linear analysis, the existence of the Lyapunov function $\mathcal{L} = \lambda[a_r \ln a(t) + b_r \ln b(t) - a(t) - b(t)]$ for the rate equations (2) and (4) implies the global stability of the reactive fixed point (a_r, b_r) [6, 8].

Thus already within the mean-field approximation a finite prey carrying capacity ρ, which can be viewed as the average result of local restrictions on the B density, drastically affects the phase diagram by inducing an extinction threshold (at λ_c for fixed μ) for the predator population. Taking spatial fluctuations into account, this becomes a genuine continuous active-to-absorbing phase transition for the A species. It is now well established that its critical properties are governed by the scaling exponents of directed percolation, with critical dimension $d_c = 4$ (see [24] and references therein).

3. Monte Carlo simulations

3.1. Data structure

Monte Carlo simulations of chemical kinetics on a lattice are usually performed with site occupation number restrictions (e.g., any lattice site may be occupied by at most one particle of either species) since this situation is readily coded in a straightforward and efficient manner. Indeed, for any stochastic simulation of chemical kinetics, a lack of site restrictions presents a challenge for efficient algorithms and data storage. Unlike the restricted case, no upper bound can be placed on the number of occupants of a lattice site. Thus, the memory structure must be made to follow the particles interacting on the lattice rather than just the lattice itself. This requirement calls for a more dynamic implementation of the simulation than simply flipping bits on a two-dimensional array.

In this subsection, we briefly overview several approaches to storing the particle information, and compare them in light of a decomposition of the demands the simulation will place on the data structure. We then present and explain the hybrid data structure utilized in our simulations. In essence, simulating diffusing and interacting particles on a lattice requires four operations repeated in different combinations, namely

(i) Random selection: a lattice occupant is selected at random with a uniform probability, which allows for the simulation to proceed in an unbiased manner.
(ii) Query: this operation determines the number of particles of any species located on a given site at a specific instant; it is desirable to render this operation fast, which puts some constraints on the particle ordering in the data structure.
(iii) Add: a new particle is inserted into the lattice.
(iv) Remove: annihilates a particle from the lattice; a particle movement can be implemented as sequential Remove and Add.

Considering these operations provides us with a frame in which to compare the competing data structures and algorithms for implementing site-unrestricted stochastic lattice simulations for particle reactions.

The first such candidate, a static array, is perhaps the most intuitive. In this implementation, we simply construct arrays (in arbitrary d dimensions) of integer n-tuples, where each integer tells how many particles of a given species currently reside on this site. The problem of unbound variables is avoided by imposing some loose site restrictions, say by setting a cap of some large maximum number M of particles per site. Such a restriction would be irrelevant to the chemical kinetics unless we actually encounter such a large number on a single site, which is typically not likely. However, this implementation presents major problems with random selection. When restriction is in place, especially strong restrictions, such as allowing only a single occupant per site, the typical algorithm proceeds by selecting sites at random repeatedly until an occupied one is found. This can be duplicated for any site restriction, including very loose ones. However, with L^d sites, N occupants, and a site restriction of M particles per site,

this algorithm has a time complexity of $O(L^d M/N)$, and is thus very inefficient for very large M. A more reliable algorithm, albeit still relatively slow, involves a full traversal of the lattice; therefore, the best we can do here is $O(L^d)$.

The next possible candidate is an unordered list with random access. This implementation would simply construct a very long list at the beginning of the simulation, and then proceed to populate it with the lattice occupants, where each entry keeps track of its own location in the lattice. This structure gives very fast random selection, insertion, and removal, all O(1). However, since it is unordered, a query could easily require searching the entire list, which results in an $O(N)$ performance for the query. We might try to enhance the query performance by ordering the list or constructing it as a tree; in either case the search efficiency is improved to $O(\log N)$. But we also degrade the insertion and removal to $O(\log N)$. In the process, if we have constructed these data structures within the confines of an array so that we can maintain random access, random selection remains sufficiently fast, at O(1). However, if we lose random access, as in the traditional linked list or binary search tree, we arrive at $O(N)$ complexity for the random selection, since any random selection would require an ordered traversal of the tree or list.

Therefore, the data structure we propose hybridizes the first two candidates above to ensure constant time complexity for each of the necessary operations. What is required is to use a spatial array to allow fast addition, removal and queries, but to manage the memory in such a way as to provide random access to an unordered list of the occupants of the sites, therefore enabling immediate access for the uniformly random selection of an occupant. To accomplish this hybridization, we keep an unordered list of all the current occupants of the lattice. Each of these maintains information about where in the lattice it is located. In turn, we maintain a spatial array of the lattice, where each site contains a pointer to the head of a linked list of occupants. The fact that these occupants are stored within the global, unordered list imposes no constraint on our ability to render them elements of local linked lists. If for a given simulation it is desired to maintain unique information about each individual lattice occupant apart from its location, then this implementation does require some traversal of the site-local linked lists. This can become quite burdensome as the expected occupancy of a site grows. Yet if we can sacrifice such individual information, we need only ever interact with the head of each site-local list, or an occupant that we have already found directly through the random selection. Thus, constant time complexity can be maintained.

3.2. Monte Carlo simulation procedure

For each iteration of the simulation, a lattice occupant (either predator or prey) is selected at random, and hops to a nearest-neighbour site, and may subsequently be subjected to an (on-site) reaction. To keep track of the evolution of the system through time t, each such step is accompanied by an increment in time equal to $1/N(t)$, where $N(t)$ is the total number of occupants at this instant. In this way, in a single time step, on average every occupant has been once selected for interaction.

Our specific Monte Carlo simulation for the unconstrained stochastic lattice Lotka–Volterra model proceeds as follows:

(i) Select a lattice occupant at random.
(ii) Select one of the $2d$ sites (on a hypercubic lattice in d dimensions) adjacent to this occupant, and move it there (nearest-neighbour hopping).
(iii) If the occupant is a B particle (prey) generate a random number r_1 over the range $[0, 1)$; if $r_1 < \sigma$, add another new B particle to the current site (prey offspring production, $B \rightarrow B + B$).

(iv) If the occupant is an A particle (predator)

(a) if there are any B particles (prey) located on this site: for *each* B particle generate a random number r_2 over the range [0, 1); if $r_2 < \lambda$, remove it from and add one new A particle to this site (predation interaction, $A + B \to A + A$);

(b) generate a random number r_3 over the range [0, 1); if $r_3 < \mu$, remove this A particle (predator death, $A \to \emptyset$).

In our simulations, none of the possible events are mutually exclusive; in particular, particle diffusion and on-site reactions can happen simultaneously. Therefore, the hopping probability is held fixed at unity for the entire range of reaction parameters, which obviates the need for renormalization of the simulation time for different reaction rates. Notice that in contrast with site-restricted simulations, where offspring particles need to appear at neighbouring sites, which causes either species to propagate in space, here hopping processes have to be put in explicitly. All simulation runs reported below start from random initial spatial distributions of both predators A and prey B. We have also run simulations where step iv (a) above was modified: instead of exposing each prey on a given site to predation by the invading predator, we allowed only at most a single B particle to be removed.

4. Simulation results

4.1. Spatio-temporal structures and spatial correlations in two dimensions

Figure 2 depicts a set of snapshots from a simulation on a 256×256 square lattice, run with rate parameters $\sigma = 0.1$, $\mu = 0.1$, and $\lambda = 0.1$.[3] Starting from a random (Poisson) distribution of particles A and B (a), initially the predator population goes almost extinct, with a few localized specks of prey surviving. When predators encounter the regions inhabited by the prey, they rapidly devour them, and subsequently die out (c)–(e). Eventually, the system settles in a dynamic steady state governed by expanding, competing, and merging diffuse activity fronts, forming complex spatio-temporal structures (f). This temporal evolution resembles that observed in simulations with restricted site occupation numbers deep in the species coexistence phase (compare, e.g., figure 2 in [24] and footnote 3), except that the fronts are more diffuse in the unrestricted simulations, broadened by regions that contain both predators and prey (colour-coded magenta/light grey). Yet there is also a marked difference, namely the predator–prey competition is far more local and thus considerably faster in the present simulation runs.

The emerging spatial structures can be characterized quantitatively through the static (and translationally invariant) correlation functions $C_{\alpha\beta}(x) = \langle n_\alpha(x) n_\beta(0)\rangle - \langle n_\alpha\rangle\langle n_\beta\rangle$, where $\alpha, \beta =$ A, B, and $n_\alpha(x)$ denotes the occupation number for particle species α at site x. Figure 3 depicts the results for $C_{AA}(x)$ (a), $C_{BB}(x)$ (b), and $C_{AB}(x)$ (c), as obtained from Monte Carlo simulations on a 1024×1024 square lattice, with rates $\sigma = 0.1$, $\mu = 0.1$, and various values of the predation rate $\lambda = 0.5$, 0.75, and 1.0. Each set of measurements was initiated in a well developed simulation, having run for 3000 time steps, which was subsequently performed for an additional 1000 time steps, while sampling the state of the system every 25 steps. Thus, the correlation results are averaged over 40 separate times throughout the 1000 additional steps. The log–linear plots for $C_{AA}(x)$ and $C_{BB}(x)$ capture the essentially exponentially decaying correlations of particles of the same species. This suggests the form

[3] Two movies obtained from simulations on 256×256 square lattices with periodic boundary conditions and random initial distributions are accessible at http://www.phys.vt.edu/~tauber/PredatorPrey/movies/, namely for the sets of rates $\sigma = 0.1$, $\mu = 0.1$, $\lambda = 1.0$, and $\sigma = 0.5$, $\mu = 0.5$, $\lambda = 1.0$, along with several runs for restricted site occupation numbers.

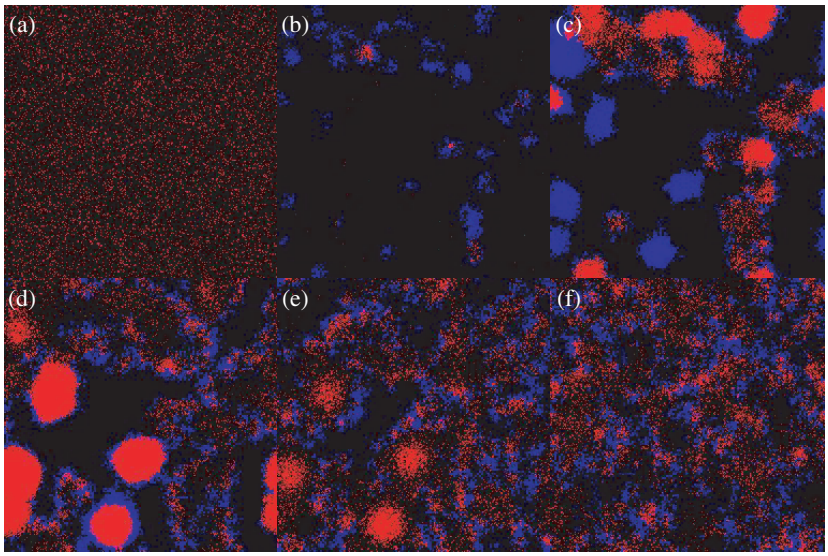

Figure 2. Snapshots taken from a simulation on a 256 × 256 lattice, with rates $\sigma = 0.1$, $\mu = 0.1$, and $\lambda = 1.0$. Light (red) and grey (blue) pixels respectively indicate sites with at least one predator (A) and prey (B); dark grey (magenta) sites are occupied by at least one representative of either species; black sites are empty. The simulation proceeds from (a) to (f), with pictures taken at time $t = 0$, 50, 95, 129, 170, and 600.

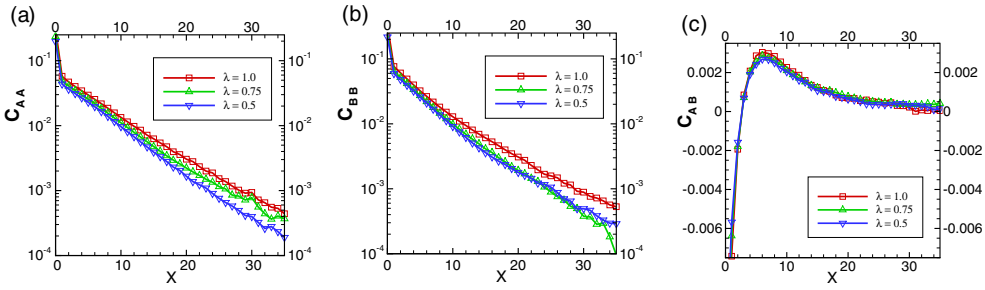

Figure 3. Static correlation functions (a) $C_{AA}(x)$, (b) $C_{BB}(x)$, and (c) $C_{AB}(x)$, measured in simulations on a 1024 × 1024 lattice, with rates $\sigma = 0.1$, $\mu = 0.1$, and with λ varied among 0.5 (blue triangles, upside-down), 0.75 (green upright triangles), and 1.0 (red squares).

$C_{AA}(x) \propto C_{BB}(x) \approx F e^{-|x|/\xi}$, with equal correlation lengths ξ for the predators and prey; in addition, both ξ and the amplitude F appear to depend only weakly on the predation rate. Qualitatively similar (but quantitatively different) to simulations with restricted site occupation numbers (compare figure 4 in [24]), in figure 3(c) we observe local anti-correlations between the A and B species for $0 \leqslant x \leqslant 2$, which are of course caused by the predation reaction. There are pronounced positive correlations up to about 20 lattice constants, which indicates the width of the rather diffuse predator–prey activity fronts seen in figure 2.

4.2. Population oscillations

When the predator and prey total population densities $a(t)$ and $b(t)$ are plotted as functions of time t, one finds marked oscillations in the early time regime, as shown for two examples in

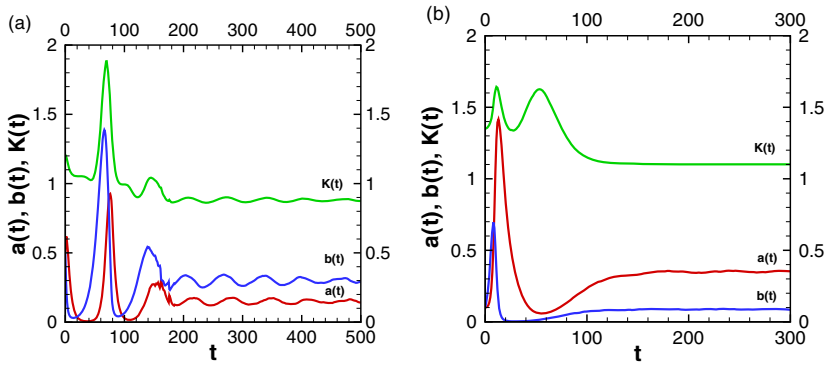

Figure 4. Early time evolution for the population density of predators $a(t)$ (red), prey $b(t)$ (blue), and the quantity $K(t)$ (green) defined in (3) from two single runs on a 1024×1024 lattice, both starting with a random distribution with rates (a) $\sigma = 0.1$, $\mu = 0.2$, and $\lambda = 1.0$, and (b) $\sigma = 0.4$, $\mu = 0.1$, and $\lambda = 1.0$.

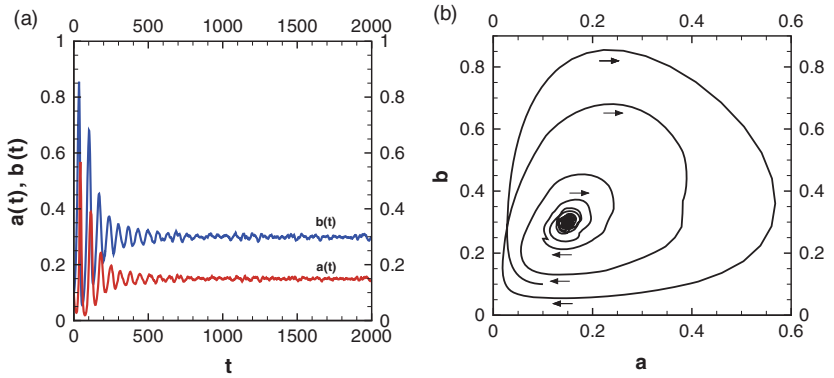

Figure 5. (a) Predator $a(t)$ (red) and prey $b(t)$ (blue) densities versus time in a simulation run on a 1024×1024 lattice, with random initial distribution, and rates $\sigma = 0.1$, $\mu = 0.2$, $\lambda = 1.0$, and initial densities $a(0) = b(0) = 0.1$. (b) Trajectory in the a–b plane from the simulation data shown in (a), up to $t = 1000$.

figure 4. These stochastic oscillations reflect the recurrent spatio-temporal structures visible in figure 2. As time progresses, the amplitude of these transient fluctuations decreases considerably, but, as in simulations with site restrictions, in finite systems these transient oscillations may persist for a long time; see also figure 5(a) below. Increasing the reaction rates (with the hopping rate fixed) effectively renders the processes more local, which suppresses front spreading and consequently reduces the amplitude of the population oscillations, as evident in figure 4(b). In order to compare with the deterministic rate equations, we have also plotted the quantity $K(t)$ defined in (3), which according to the mean-field approximation would remain constant. Yet, we see that it in fact oscillates roughly in phase with the particle densities: fluctuations evidently *amplify* at least the initial population cycles. It is important to note that (in the thermodynamic limit) the asymptotic long-time mean population densities as well as $K(t \to \infty)$ are determined by the reaction rates, and become *independent* of their initial values, as is confirmed in figure 4.

As already apparent from the analysis of the corresponding rate equations, in systems with limited prey carrying capacity an extinction threshold for the predator population appears at

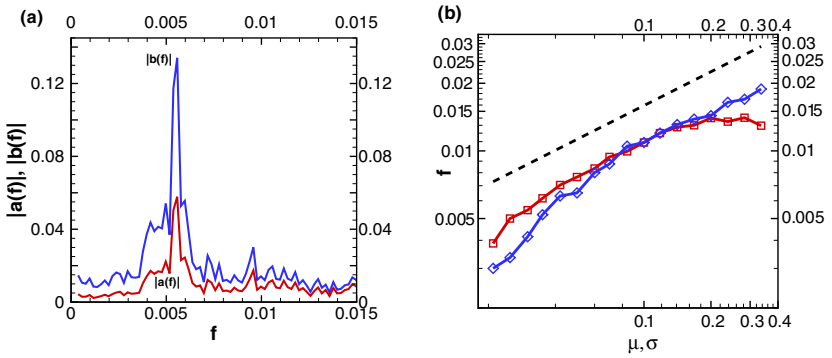

Figure 6. (a) Fourier transforms $|a(f)|$ and $|b(f)|$ of the predator (red) and prey (blue) density data for a simulation run on a 1024×1024 lattice with rates $\sigma = 0.03$, $\mu = 0.1$, and $\lambda = 1.0$, as a function of frequency f. (b) Variation of the characteristic peak frequencies in $|a(f)|$ and $|b(f)|$ with σ (red squares) and μ (blue diamonds), with the respective other rate held fixed at the value 0.1 and $\lambda = 1.0$, as obtained from simulation data on 1024×1024 lattices up to time $t = 20\,000$, compared with the result $f = \sqrt{\mu\sigma}/2\pi$ from (linearized) mean-field theory (black dashed).

sufficiently low values of the predation rate λ (with σ and μ held fixed). We have investigated our lattice model with (almost) unlimited prey occupation number in the limit of low values of λ, down to $\lambda \approx 0.02$, and found no signature of any phase transition: in the thermodynamic limit, this unconstrained predator–prey system seems to always allow species coexistence (as usual, however, *finite* systems should terminate in the absorbing state, albeit after potentially enormous crossover times). Neither have we encountered a situation where the stable species coexistence regime is governed by a stable node fixed point, which would be approached without any population oscillations; however, as mentioned before, for higher reaction rates the oscillations become strongly damped. Figure 5 depicts the population densities for an extended simulation run with rates $\sigma = 0.1$, $\mu = 0.2$, $\lambda = 1.0$, and initial values $a(0) = b(0) = 0.1$ (well away from the steady-state densities), along with the corresponding phase space trajectory in the a–b plane, which should be compared with the mean-field pictures in figure 1, computed with the same rates. Obviously, the initial state determines only transient behaviour; the long-time regime is governed by stochastic fluctuations about the attractive fixed point in the centre of the graph. We expect these to be quite well described by the zero-dimensional effective urn model and the 'resonant amplification' mechanism described in [22].

Additional information can be extracted from the simulation data by studying the (fast) Fourier transforms $a(f) = \int a(t)\mathrm{e}^{2\pi \mathrm{i} f t}\,\mathrm{d}t$ and similarly $b(f)$ of the time signals $a(t)$ and $b(t)$. As shown in figure 6 for runs with $\sigma = 0.03$, $\mu = 0.1$, and $\lambda = 1.0$, extended to $t = 20\,000$, the predator and prey Fourier signals display prominent peaks at the same characteristic frequency, which evidently governs the erratic oscillations. In order to assess the validity of the linearized mean-field approximation result $f = \sqrt{\mu\sigma}/2\pi$ quantitatively, we have obtained the peak frequency values for various Monte Carlo simulations on 1024×1024 square lattices, all run with $\lambda = 1.0$ and with either μ or σ held fixed at the value 0.1, while the respective other rate is varied between 0.02 and 0.36. The results are displayed as a double-logarithmic plot in figure 6(b). Interestingly, the simulation data show a more pronounced deviation from the square-root dependence on μ than on σ for low rates, while the reverse is true for large rates. Moreover, the characteristic peak frequencies are reduced by about 50% as compared with the mean-field prediction, obviously renormalized by stochastic fluctuations; similar effects are found in site-restricted simulations (see figure 9 in [24]). It is remarkable

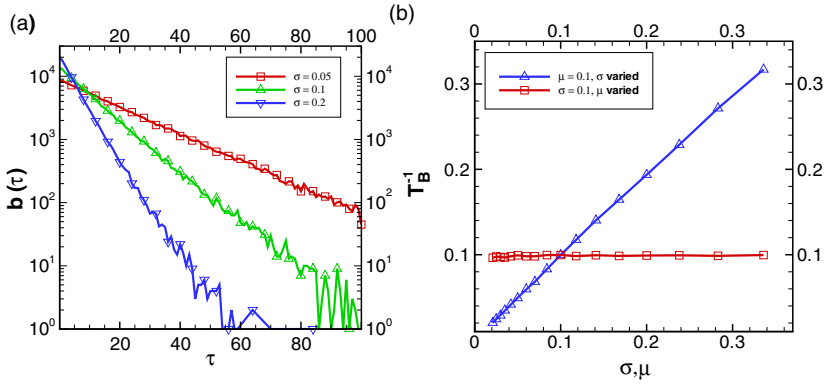

Figure 7. (a) Prey age distribution histogram $b(\tau)$ as a function of their lifetime τ, obtained from Monte Carlo simulations on a 1024×1024 lattice with $\mu = 0.1$, $\lambda = 1.0$, and $\sigma = 0.05$ (red squares), 0.1 (green upright triangles), and 0.2 (blue triangles, upside-down). (b) Inverse mean prey lifetimes T_B^{-1} as measured in similar simulations, with fixed $\lambda = 1.0$ and either σ (blue triangles) or μ (red squares) varying, and the respective other rate held constant at 0.1.

though that for values between 0.04 and 0.24 the curves for varying rates μ or σ appear to coincide, which would indicate the simple functional dependence $f(\mu, \sigma) = \tilde{f}(\mu\sigma)$ in this range.

4.3. Age distributions

We have also obtained the age histograms $b(\tau)$ for the total number of surviving prey up to time τ after they were produced. The log–linear plot in figure 7(a), taken for $\mu = 0.1$, $\lambda = 1.0$, and different values of $\sigma = 0.05, 0.1, 0.2$ on a 1024×1024 square lattice, shows that the prey age distribution $b(\tau)$ essentially decays exponentially with τ. From the slopes in these graphs we can read off the prey population inverse mean lifetime T_B^{-1}, which is plotted in figure 7(b) as a function of the rates σ (with $\mu = 0.1$ and $\lambda = 1.0$ held fixed), and as a function of μ ($\sigma = 0.1$, $\lambda = 1.0$). One finds that $T_B^{-1}(\sigma, \mu) \approx \sigma$ for the rate interval studied here, whereas it displays no markedly significant dependence on μ. This is indeed borne out already upon linearizing the mean-field rate equations (2) about the steady state ($a_u = \sigma/\lambda, b_u = \mu/\lambda$), which yields an effective prey death rate σ induced by the predation reaction, independent of μ.

4.4. One-dimensional simulations

We have also run Monte Carlo simulations for our unconstrained lattice Lotka–Volterra model in one dimension. The total population densities as well as space–time plots for the first 500 time steps are shown for two representative examples in figures 8 and 9. In the first run, the reaction rates are low (all 0.01), and the kinetics is dominated by diffusion. Correspondingly, the system remains well mixed, and displays a stochastic time signal. In the second simulation, with all rates set to 1.0, the on-site reactions dominate. Localized prey population bursts occur, but invading predators quickly remove emerging prey clusters, subsequently proliferate and then die out, which leads to intriguing wedge-like structures in the early time regime. At any rate, we generally observe species coexistence during the duration of our runs, in accord with earlier investigations of a one-dimensional four-state system [16]. This is in stark contrast with simulations with restricted site occupation numbers, where the system tends towards eventual predator extinction, with the asymptotic approach to the absorbing state proceeding via very

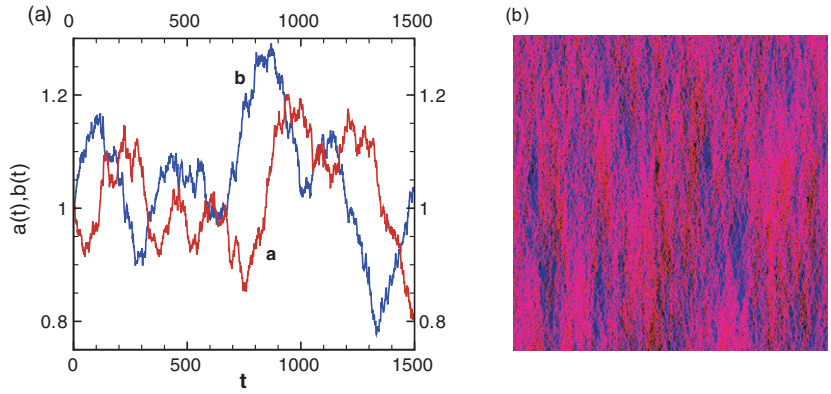

Figure 8. (a) Predator (light/red) and prey (grey/blue) population densities in a (single) one-dimensional simulation on 512 lattice sites with rates $\sigma = 0.01$, $\mu = 0.01$, $\lambda = 0.01$, and $a(0) = b(0) = 1$. (b) Space–time plot, with time running from top to bottom (up to $t = 500$) for this diffusion-dominated run, where red and blue pixels respectively indicate sites with at least one predator (A) and prey (B); magenta sites are occupied by at least one representative of either species; black sites are empty.

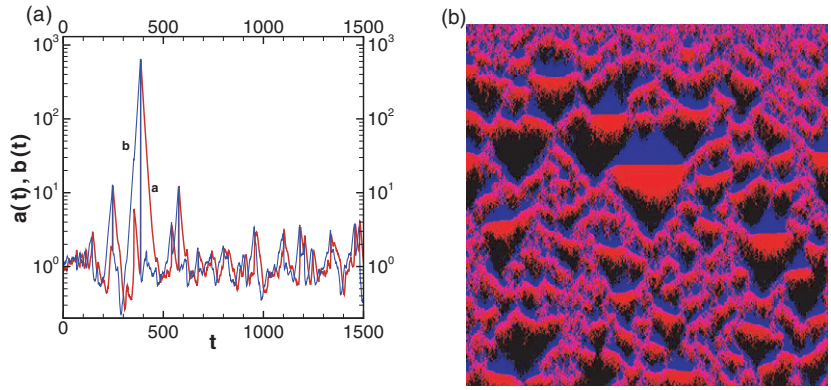

Figure 9. (a) Predator (light/red) and prey (grey/blue) population densities in a (single) one-dimensional simulation on 512 lattice sites with rates $\sigma = 0.1$, $\mu = 0.1$, $\lambda = 0.1$, and $a(0) = b(0) = 1$, and corresponding space–time plot, with time running from top to bottom (up to $t = 500$) for this reaction-dominated run.

slow coarsening processes, namely merging of the active domains, presumably governed by the $t^{-1/2}$ power law of single-species coagulation (see figure 11 in [24]).

4.5. Simulations with restricted predation

As mentioned in section 3.2, we have also performed simulations wherein an A particle in each of its moves to a new site could annihilate at most one B particle there. In effect, this sets an upper limit to the efficiency of the predation process, at variance with the rate equations (2), which induces interesting differences to the previous simulations with multiple simultaneous predation events when the prey density becomes large. At large predation rates $\lambda > \mu$, the qualitative behaviour of this model variant is essentially as described above. However, there emerges one distinction when the reaction rates are large (with the hopping rate D held fixed),

and the on-site reactive processes dominate. In this situation, instead of spreading diffuse predator–prey fronts, we have observed pulsating activity zones. In addition to the familiar erratic oscillations, these induce intermittent population spikes that tend to dominate the long-time properties of the system. (In fact, these localized population explosions set limits to the rates we could explore, because the maximum site occupation number bounds may become exceeded.)

More dramatically, when λ approaches μ from above, predation becomes too inefficient for the predators, and we find an extinction threshold for the A population at (or very near) $\lambda \approx \mu$. For $\lambda < \mu$, $a(t)$ appears to decay exponentially; at the transition, however, the predator density can apparently assume any value. A proper characterization of this unusual extinction transition would however require considerable additional effort.

5. Discussion and conclusion

Understanding biodiversity and identifying mechanisms allowing us to maintain coevolution, as well as the influence of spatial distribution of the agents, are central problems in modern theoretical biology and ecology. In this context, we have studied a stochastic lattice version of the Lotka–Volterra model for the dynamics of two competing populations. As a main difference with numerous earlier studies, we have performed Monte Carlo simulations without any site restrictions, which can be interpreted in the biological or ecological context as a system without local limitation of the growth rate. This study is also of interest from a physical viewpoint because, at the deterministic mean-field rate equation level, one naturally recovers the genuine Lotka–Volterra equations from the present stochastic model system. This investigation also allows us to test further the robustness of stochastic predator–prey systems, which have been recently shown to share numerous properties. From a biological and ecological perspective, it is relevant to understand better the role of the presence or absence of some form of spatial limitation of the resources, which can be (arguably) simply mimicked by considering site restricted and unrestricted stochastic models, respectively.

After having briefly outlined the basic features of the Lotka–Volterra model in the framework of the mean-field rate equations, both for infinite and finite carrying capacity of the prey population, and explaining the procedure we have developed to efficiently structure the data, we have reported results of extensive simulations of our unrestricted stochastic predator–prey system. As a major difference with respect to the results for site-restricted models, we have found no evidence of any extinction threshold in our one-and two-dimensional simulations. With both types of agents being allowed to locally proliferate, both species are always found to coexist. Similar to the site-restricted models deep in the coexistence phase, our unrestricted system is characterized by complex and correlated patterns emerging from 'pursuit and evasion' wavefronts. These are rendered more diffuse in the present unrestricted simulations through regions accommodating both predators and prey on the same spots. The quantitative properties (characteristic correlation lengths) of the patterns have been studied by computing various static correlation functions. The dynamical properties have been investigated by considering both time dependence of the densities and the trajectories in the phase portrait. As for restricted stochastic models, the population densities are typically characterized by damped erratic oscillations, with an amplitude that vanishes in the thermodynamic limit. However, as a novel feature, when the reaction rates dominate over the diffusive process, the reaction kinetics takes place largely locally (on site), and one observes, depending on the model variant, either quickly decaying oscillations, or pulsating activity zones and spikes in the density profiles. By means of a Fourier analysis, and similar to the restricted case, we have found that the characteristic frequency of the damped and fluctuation-induced oscillations is markedly reduced with respect

to the mean-field prediction, while its functional dependence seems in reasonable agreement with the deterministic result. We have also studied the prey age distribution and shown that it decays exponentially, with an inverse mean lifetime independent of the death rate of the predators and depending linearly on the reproduction rate of the prey.

Acknowledgments

This work was in part supported by the US National Science Foundation through grant NSF DMR-0308548. MM gratefully acknowledges the support from the German Alexander von Humboldt Foundation through fellowship IV-SCZ/1119205 STP. We would like to thank E Frey, I T Georgiev, R Kulkarni, A McKane, T Newman, S Redner, T Reichenbach, B Schmittmann, N Shnerb, and R Stinchcombe for inspiring discussions.

References

[1] Lotka A J 1920 *Proc. Natl Acad. Sci. USA* **6** 410
Lotka A J 1920 *J. Am. Chem. Soc.* **42** 1595
[2] Volterra V 1926 *Mem. Accad. Lincei* **2** 31
Volterra V 1931 *Leçons sur la Théorie Mathématique de la Lutte Pour la Vie* (Paris: Gauthiers-Villars)
[3] Haken H 1983 *Synergetics* 3rd edn (New York: Springer)
[4] May R M 1973 *Stability and Complexity in Model Ecosystems* (Princeton, NJ: Princeton University Press)
[5] Maynard S J 1974 *Models in Ecology* (Cambridge: Cambridge University Press)
[6] Hofbauer J and Sigmund K 1998 *Evolutionary Games and Population Dynamics* (Cambridge: Cambridge University Press)
[7] Neal D 2004 *Introduction to Population Biology* (Cambridge: Cambridge University Press)
[8] Murray J D 2002 *Mathematical Biology* vol I, II (New York: Springer)
[9] Matsuda H, Ogita N, Sasaki A and Satō K 1992 *Prog. Theor. Phys.* **88** 1035
[10] Satulovsky J E and Tomé T 1994 *Phys. Rev.* E **49** 5073
[11] Boccara N, Roblin O and Roger M 1994 *Phys. Rev.* E **50** 4531
[12] Durrett R 1999 *SIAM Rev.* **41** 677
[13] Provata A, Nicolis G and Baras F 1999 *J. Chem. Phys.* **110** 8361
[14] Rozenfeld A F and Albano E V 1999 *Physica* A **266** 322
[15] Lipowski A 1999 *Phys. Rev.* E **60** 5179
[16] Lipowski A and Lipowska D 2000 *Physica* A **276** 456
[17] Monetti R, Rozenfeld A F and Albano E V 2000 *Physica* A **283** 52
[18] Bettelheim E, Agam O and Shnerb N M 2001 *Physica* E **9** 600
[19] Droz M and Pekalski A 2001 *Phys. Rev.* E **63** 051909
[20] Antal T and Droz M 2001 *Phys. Rev.* E **63** 056119
[21] Kowalik M, Lipowski A and Ferreira A L 2002 *Phys. Rev.* E **66** 066107
[22] McKane A J and Newman T J 2005 *Phys. Rev. Lett.* **94** 218102
[23] Mobilia M, Georgiev I T and Täuber U C 2006 *Phys. Rev.* E **73** 040903(R)
[24] Mobilia M, Georgiev I T and Täuber U C 2006 *J. Stat. Phys.* doi:10.1007/510955-006-9146-3
(Mobilia M, Georgiev I T and Täuber U C 2006 *Preprint* q-bio.PE/0512039)
[25] Reichenbach T, Mobilia M and Frey E 2006 *Phys. Rev.* at press
[26] Hinrichsen H 2000 *Adv. Phys.* **49** 815
[27] Odor G 2004 *Rev. Mod. Phys.* **76** 663
[28] Janssen H K and Täuber U C 2005 *Ann. Phys.* **315** 147
[29] Täuber U C, Howard M J and Vollmayr-Lee B P 2005 *J. Phys. A: Math. Gen.* **38** R79